N- and C-terminal *KCNE1* mutations cause distinct phenotypes of long QT syndrome

Seiko Ohno, MD,* Dimitar P. Zankov, MD,† Hidetada Yoshida, MD, PhD,* Keiko Tsuji, MS,† Takeru Makiyama, MD,* Hideki Itoh, MD, PhD,† Masaharu Akao, MD, PhD,* Jules C. Hancox, PhD,‡ Toru Kita, MD, PhD,* Minoru Horie, MD, PhD†

*From the *Department of Cardiovascular Medicine, Kyoto University Graduate School of Medicine, Kyoto, †Department of Cardiovascular and Respiratory Medicine, Shiga University of Medical Science, Shiga, Japan, and ‡Department of Physiology, School of Medical Sciences, University of Bristol, Bristol, United Kingdom.*

BACKGROUND Long QT syndromes (LQTS) are inherited diseases involving mutations to genes encoding a number of cardiac ion channels and a membrane adaptor protein. The MinK protein is a cardiac K-channel accessory subunit encoded by the *KCNE1* gene, mutations of which are associated with the LQT5 form of LQTS.

OBJECTIVE The purpose of this study was to search for the *KCNE1* mutations and clarify the function of those mutations.

METHODS We conducted a genetic screen of *KCNE1* mutations in 151 Japanese LQTS patients using the denaturing high-performance liquid chromatography-WAVE system and direct sequencing. In two LQTS patients, we identified two *KCNE1* missense mutations, located in the MinK N- and C-terminal domains. The functional effects of these mutations were examined by heterologous coexpression with *KCNQ1* and *KCNH2*.

RESULTS One mutation, which was identified in a 67-year-old woman, A8V, was novel. Her electrocardiogram (ECG) revealed marked bradycardia and QT interval prolongation. Another mutation, R98W, was identified in a 19-year-old woman. She experienced syncope followed by palpitation in exercise. At rest, her ECG showed bradycardia with mild QT prolongation, which became more prominent during exercise. In electrophysiological analyses, R98W produced reduced I_{Ks} currents with a positive shift in the half activation voltages. In addition, when the A8V mutation was coexpressed with *KCNH2*, this reduced current magnitude, which is suggestive of a modifier effect by the A8V *KCNE1* mutation on I_{Kr}.

CONCLUSION *KCNE1* mutations may be associated with mild LQTS phenotypes, and *KCNE1* gene screening is of clinical importance for asymptomatic and mild LQTS patients.

KEYWORDS Long QT syndrome; *KCNE1*; Ion channels; Molecular screening; Electrophysiology

(Heart Rhythm 2007;4:332–340)

Introduction

Long QT syndromes (LQTS) are characterized by a prolonged QT interval in the electrocardiogram (ECG) and a high risk of sudden cardiac death due to a characteristic ventricular tachycardia known as torsades de pointes. The syndromes are hereditary based on gene mutations encoding multiple cardiac ion channels and a membrane adaptor protein.[1] In 1996, positional cloning methods established *KCNQ1* as the chromosome 11–linked LQT1 gene.[2] Subsequently, MinK, a potassium channel regulatory subunit encoded by the *KCNE1* gene,[3,4] was shown to coassemble with *KCNQ1* to produce the slowly activating delayed-rectifier K^+ current, I_{Ks}.[5,6] Because of these relationships, MinK was thought to be another candidate for LQTS. At the end of 1997, two groups first identified clinically significant *KCNE1* mutations in LQTS patients.[7,8] Schulze-Bahr and coworkers[7] reported a *KCNE1* compound heterozygous mutation, which induced the Jervell and Lange-Nielsen syndrome (JLNS). The mutations were T7I and D76N, which were located in the N terminus and C terminus of the MinK protein, respectively. Splawski and coworkers[8] also reported two families of the Romano-Ward syndrome and identified two C-terminal *KCNE1* mutations, S74L and D76N. In functional analyses, D76N caused a decreased I_{Ks} current with a strong dominant-negative effect. On the other hand, S74L also decreased I_{Ks} but displayed no dominant-negative effect. Further investigation confirmed the *KCNE1* gene as the fifth LQTS locus (LQT5).[9]

To date, 16 LQT5-related *KCNE1* mutations have been reported, but this number and the incidence of mutations are very small compared with the principal LQTS mutations (LQT1-3). The functional consequences of *KCNE1* mutations in reducing I_{Ks} vary considerably between mutations. Furthermore, the gene-specific phenotype has not been well investigated in LQT5. Here we report two *KCNE1* mutations identified in two Japanese LQTS patients from unre-

MH was supported by Research Grants from the Japan Ministry of Education, Science, Sports and Culture and by Health Science Research Grants from the Japan Ministry of Health, Labor, and Welfare. **Address reprint requests and correspondence:** Minoru Horie, M.D., Ph.D., Department of Cardiovascular and Respiratory Medicine, Shiga University of Medical Science, Seta Tsukinowa-cho, Otsu, Shiga, Japan 520-2192. E-mail address: horie@belle.shiga-med.ac.jp. (Received August 12, 2006; Accepted November 1, 2006.)

1547-5271/S -see front matter doi:10.1016/j.hrthm.2006.11.004

lated families, which are located in the N terminus and C terminus. Although these patients had no mutations in LQTS-related genes other than *KCNE1* and relatively mild LQTS phenotypes, the response of QT intervals to heart rates was quite different: QT prolongation became prominent in bradycardia with the N-terminal mutation (A8V) and in tachycardia with the C-terminal mutation (R98W). These heart rate dependencies were compatible with the symptoms of reducing I_{Kr}–rapidly activating delayed-rectifier K^+ current–and I_{Ks}, respectively. Since MinK is also able to coassemble with the HERG protein (encoded by *KCNH2*) and affect the I_{Kr} current,[10–12] we examined the functional influence of these two mutations on both *KCNQ1*- and *KCNH2*-encoded channels, using a heterologous expression system. In this report, we first displayed novel phenotypes of LQT5 that would be caused by reduced I_{Kr}.

Methods

Subjects

The cohort of patients studied was comprised of 151 consecutive LQTS probands showing prolongation in the QT interval (QTc ≥ 460 ms); they were referred to our laboratory for genetic evaluation from all over Japan. The patients had both familial and acquired LQTS. All subjects gave their written informed consent in accordance with guidelines approved by the appropriate institutional review boards. Each underwent detailed clinical and cardiovascular examinations and was then characterized phenotypically on the basis of the QT interval in lead V_5, corrected for heart rate (QTc) according to Bazett's formula, and the presence of cardiac symptoms. Schwartz's scores[13] of all probands were greater than 3 points.

Genotyping

Genomic DNA was isolated from venous blood by use of the QIAamp DNA blood midikit (Qiagen, Hilden, Germany). Established primer settings were employed to amplify the entire coding regions of the known LQTS genes (*KCNQ1*,[14,15] *KCNH2*,[14] *SCN5A*,[16] *KCNE1*,[14] and *KCNE2*[17]), with the exception of *ANKB*[18] from genomic DNA. The denaturing high-performance liquid chromatography (DHPLC; WAVE system Model 3500, Transgenomic, Omaha, NE) technique was performed as described elsewhere.[19] Polymerase chain reaction (PCR) products were denatured at 95°C for 5 minutes and then analyzed in DHPLC. The PCR fragments presenting abnormal signals in DHPLC analysis were subsequently sequenced by the dideoxynucleotide chain termination method with fluorescent dideoxynucleotides on an ABI 3100 genetic analyzer (PE Applied Biosystems, Foster City, CA).

Site-directed mutagenesis and expression

Complementary DNAs (cDNAs) for human *KCNQ1* (GenBank AF000571) and *KCNE1* (GenBank M26685) were kindly provided by Dr. J. Barhanin (Institut de Pharmacologie Moléculaire et Cellulaire, CNRS, Valbonne, France). The cDNAs were subcloned into pIRES2-EGFP (for *KCNQ1*) and pIRES-CD8 (for both wild-type [WT] and mutated *KCNE1*) vectors, respectively. The cDNAs for human *KCNH2* (GenBank AF363636) were kindly gifted by Dr. M. Sanguinetti (University of Utah, Salt Lake City, UT). The cDNA was subcloned into the pCEP4/CMV vector. MinK mutations were constructed using a Quick Change II XL Site-Directed Mutagenesis Kit according to the manufacturer's instructions (Stratagene, La Jolla, CA). Nucleotide sequence analysis was performed on each variant construct before the expression study. COS7 cells were transiently transfected using 1 μg of pIRES-CD8/*KCNE1* (WT or mutants) and 1 μg of pIRES2-EGFP/*KCNQ1* per 35 mm dish, using fugene6 according to the manufacturer's instructions (Roche Diagnostics, Basel, Switzerland). CHO cells were cotransfected using 1 μg of pIRES-CD8/*KCNE1* (WT or mutants), 1 μg of pCEP4/CMV/*KCNH2* vector, and 0.5 μg of pEGFP-N1/CMV vector to detect the cells with *KCNH2* expression. COS7 or CHO cells that are successfully transfected with *KCNQ1* or *KCNH2* and *KCNE1* cDNAs were selected by green fluorescence and decoration with anti-CD8 antibody-coated beads (Dynabeads CD8; Dynal Biotech, Oslo, Norway).

Electrophysiological experiments and data analysis

Whole-cell patch-clamp recordings were made with pipettes filled with (in mM) KCl 130, KOH 20, Mg-ATP 5, Na-GTP 0.1, EGTA 5, and HEPES 10 (pH 7.2 with KOH), with a resistance of 2.0 to 4.0 MΩ. The external superfusate contained (in mM) NaCl 140, KCl 5.4, $MgCl_2$ 0.5, $CaCl_2$ 1.8, NaH_2PO_4 0.33, glucose 5.5, and HEPES 5 (pH 7.4 with NaOH). Data were filtered at 2 kHz.

Experiments on *KCNQ1* were performed at 37°C using an Axopatch 200A patch-clamp amplifier (Axon Instruments, Foster City, CA) 48–72 hours after transfection. PClamp software (version 9.0, Axon Instruments) was used to generate voltage pulse protocols and for data acquisition. Currents were elicited by depolarizing pulses from a holding potential of −70 mV to test potentials between −50 and +100 mV (with a 10-mV step increment), followed by repolarization to −30 mV to monitor tail current amplitude. Current densities (pA/pF) were calculated for each cell studied by normalizing peak tail current amplitude to cell capacitance. Activation curves were derived from tail currents at −30 mV after stepping to test potentials ranging from −50 to +100 mV.

Whole-cell patch-clamp recordings with *KCNH2* were performed at 37°C using an EPC-8 patch-clamp amplifier (HEKA, Lambrecht, Germany) 48–72 hours after transfection. Data acquisition was performed using PatchMaster acquisition software (HEKA). Currents were elicited by depolarizing pulses from a holding potential of −80 mV to test potentials between −40 and +50 mV (with a 10-mV step increment), followed by repolarization to −60 mV to monitor tail current amplitude. Current densities (pA/pF) were calculated for each cell studied by normalizing peak tail current amplitude to cell capacitance. Activation curves

were derived from tail currents at −60 mV after stepping to test potentials ranging from −40 to +50 mV.

Current voltage relations were fitted with a Boltzmann's function:

$$I_{K,tail} = 1/\{1 + \exp[(V_{1/2} - V_m)/k]\} \quad (1)$$

where $V_{1/2}$ stands for the potential at which the activation is half maximal, V_m is the test potential, and k is the slope factor.

Time constants describing current time courses were obtained by data with single or double exponential functions shown below (equation 2 for single exponential and equation 3 for double exponential):

$$I(t) = A + B\exp(-t/\tau) \quad (2)$$

$$I(t) = A + B\exp(-t/\tau_{fast}) + C\exp(-t/\tau_{slow}) \quad (3)$$

where $I(t)$ means the current amplitude at time t, A, B, and C are constants, and τ refers to the activation/deactivation time constants obtained.

Numerical data are presented as mean ± standard error of the mean. Student's t-test was used to compare data between different groups for electrophysiological measurements. $P < .05$ was considered statistically significant.

Results

Mutation analysis

In 151 LQTS patients from unrelated families, we found two major elution patterns (Figures 1A(a) and 1A(b).) and two abnormal patterns (Figures 1A(c) and 1A(d)) in DHPLC analyses for *KCNE1*. Subsequent DNA sequencing revealed that the wave patterns shown in Figures 1A(a) and 1A(b) were derived from the normal and D85N polymorphism.[20–23] There were 11 patients with heterozygous D85N polymorphism. The third elution pattern (Figure 1A(c)) turned out to be due to a single nucleotide change (23C > T), causing an amino acid substitution denoted A8V, replacing an alanine at residue 8 with a valine (Figures 1B and 1C). The bottom pattern (Figure 1A(d)) was due to a single nucleotide alternation (292C > T) resulting in an amino acid substitution from an arginine at residue 98, designated R98W (Figures 1B and 1D). Both types of aberrant bands were absent in 110 unrelated healthy individuals of the general population. These mutations are located in the N terminus (A8V) and in the C terminus (R98W), respectively (shown schematically in Figure 1B). The two probands carrying *KCNE1* mutations had homozygous G38 and D85 alleles in *KCNE1* and no other mutations in the LQTS-related genes (see the Methods section). Regarding other LQTS-related genes in our cohort, we found 20 mutations from 27 patients in *KCNQ1*, 33 mutations from 37 patients in *HERG*, and 12 mutations from 12 patients in *SCN5A*.

Phenotypic characterization: Case 1

The A8V mutation was identified in a 67-year-old female who had no family history of syncope and premature sudden death. Arrhythmia was initially detected at age 63 years, and

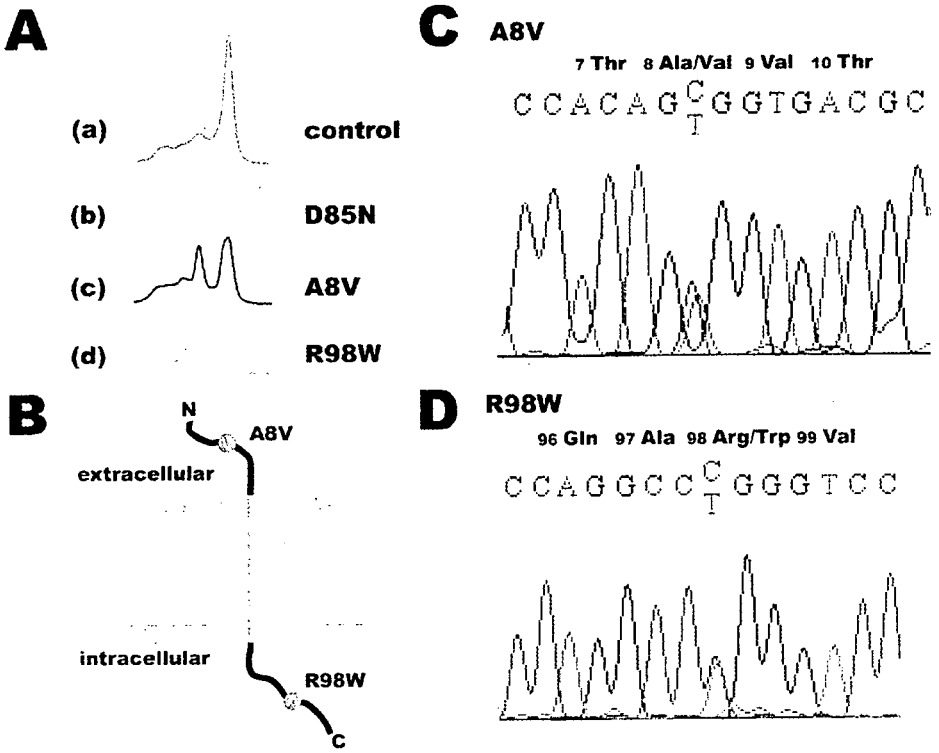

Figure 1 Mutation analysis of *KCNE1*. **A:** DHPLC analyses of PCR products amplifying *KCNE1*: from top to bottom, (a) control, (b) D85N (single nucleotide polymorphism), (c) A8V and (d) R98W. The control displayed one normal peak pattern; in contrast, D85N, A8V and R98W displayed two to four peak patterns. **B:** Location of *KCNE1* mutations. **C** and **D:** Sequence analyses for A8V and R98W.

1 month before entering the hospital she began to feel general malaise and palpitations with skipped beats. Her 12-lead ECG (Figure 2A(a)) showed prominent sinus bradycardia (46 bpm) and marked QT prolongation (QTc 600 ms) with flat and biphasic T waves in chest leads. After further examination in hospital, paroxysmal atrial fibrillation (AF; Figure 2A(b)) and sinus pause after cessation of AF were detected and were considered to be the cause of her palpitations. Under the diagnosis of bradycardia-tachycardia syndrome, she received a pacemaker implantation. With atrial pacing at 60 bpm, her QTc interval was shortened to within the normal range (QTc 428 ms; Figure 2A(c)).

Phenotypic characterization: Case 2

The R98W mutation was found in a 19-year-old female, an athlete in high school, who experienced several episodes of short-term syncope followed by palpitation during exercise at age 16. In a medical checkup, conducted at the time of entrance to college, sinus bradycardia (heart rate 45 bpm) and mild QT prolongation (QTc 460 ms) were detected on ECG. She was referred for further examination and, during and after a treadmill exercise test (Figures 2B(a) and 2B(b)), her QTc interval prolongation became more prominent. The QTc after 3 minutes of recovery was still prolonged to 580 ms, and a premature ventricular complex was observed (Figure 2B(b)). None of her relatives had a history of syncope or cardiac sudden death.

We were unable to conduct genetic analyses for the relatives of these two index patients because none of them gave informed consent.

Biophysical assays of WT and mutant *KCNE1* channels

To assess the functional consequences of these missense *KCNE1*mutations (A8V and R98W) on the MinK protein, we coexpressed WT and mutant *KCNE1*with either *KCNQ1* or *KCNH2* (Figures 3 and 4).

The C-terminal *KCNE1* mutation causes a loss of function of *KCNQ1* channels

Figure 3A shows representative families of current traces recorded from COS7 cells cotransfected with *KCNQ1* and WT or mutant *KCNE1*. Cells expressing WT-*KCNE1*/*KCNQ1* (Figure 3A, left) elicited vigorous outward currents with slow activation/deactivation kinetics, which are typical of I_{Ks} currents as reported elsewhere.[5,6] Cells expressing A8V-*KCNE1/KCNQ1* (Figure 3A, middle) revealed different voltage dependence of current activation, although the current amplitude was comparable to that of WT- *KCNE1*. In contrast, R98W-*KCNE1/KCNQ1* caused reduced currents compared with WT-*KCNE1* (Figure 3A, right). In the panel of Figure 3, the mean tail current densities measured at −30 mV in multiple measurements were shown plotted as a function of test pulse voltages (between −50 and +100 mV). Mean current densities after the depolarizing test pulse to +20 mV (indicated by arrow) were 12.4 ± 1.8 pA/pF in WT (closed circles), 11.0 ± 1.3 pA/pF in A8V (open circles), and 6.3 ± 1.2 pA/pF in R98W (closed triangles), respectively. Therefore, compared with the WT I_{Ks} channels, R98W (but not A8V) mutant channels carried significantly smaller currents on repolarization from the physiological range of action potential plateau level ($P < .05$ between WT and R98W).

To determine whether or not these mutations altered the voltage dependence of current activation, tail current densities after each test potential were normalized to the maximum value obtained after the test pulse to +100 mV. In Figure 3C, normalized currents were then plotted as a function of test potentials. The curve fits to plotted data points were obtained using equation 1 (see the Methods section). The $V_{1/2}$ and k values derived from these fits were, respectively, +40.0 ± 4.8 and 20.0 ± 1.3 mV for WT, +49.0 ± 4.3 and 23.0 ± 0.8 mV for the A8V mutation, and +55.7 ± 3.8 and 20.4 ± 1.0 mV for R98W mutation. Thus, the A8V produced a positive shift of $V_{1/2}$ by +9 mV (NS vs. WT) and R98V by +16 mV ($P < .05$ vs. WT). Effective outward currents through R98W channels were therefore reduced over a voltage range relevant to the ventricular action potential plateau level.

Time constants for both activation and deactivation were fitted to equation 2 (Methods). In comparison with WT, A8V did not influence the rate of activation, and R98W rather slowed it but there was no statistical significance. τ values at + 40 mV were 1.72 ± 0.31 seconds for WT, 1.55 ± 0.13 seconds for A8V, and 3.20 ± 0.84 seconds for R98W. τ values for deactivation at −30 mV after test pulse to 40 mV were also comparable and were 0.59 ± 0.05 seconds for WT, 0.46 ± 0.03 seconds for A8V, and 0.46 ± 0.04 seconds for R98W.

The N-terminal *KCNE1* mutation causes a loss of function of *KCNH2* channels

Figure 4A shows representative current traces recorded from CHO cells successfully cotransfected with WT or mutant *KCNE1* and *KCNH2*. Cells expressing WT and R98W *KCNE1/KCNH2* displayed outward currents with inward rectifying properties (a decline in current during the voltage command at positive test potentials), which are typical of I_{Kr} currents as reported elsewhere (Figure 4A, left and right).[24] In contrast, the magnitude of currents from cells expressing A8V-*KCNE1/KCNH2* was reduced (Figure 4A, middle). In Figure 4B, the tail current densities at −60 mV in multiple cells are plotted as a function of test pulse voltages (between −40 and +50 mV). The mean current densities after depolarizing test pulse to +20mV (indicated by arrow in graph) were 85.0 ± 13.4 pA/pF in WT (closed circles), 47.7 ± 6.9 pA/pF in A8V (open circles; $P < .05$ vs. WT), and 75.8 ± 13.8 pA/pF in R98W (closed triangles, NS vs. WT). Therefore, A8V mutant channels carried significantly smaller currents on repolarization from the physiological range of action potential plateau level.

Tail current densities after each test potential were normalized to the maximum value obtained after depolarization to +50 mV. Normalized currents thus calculated are shown

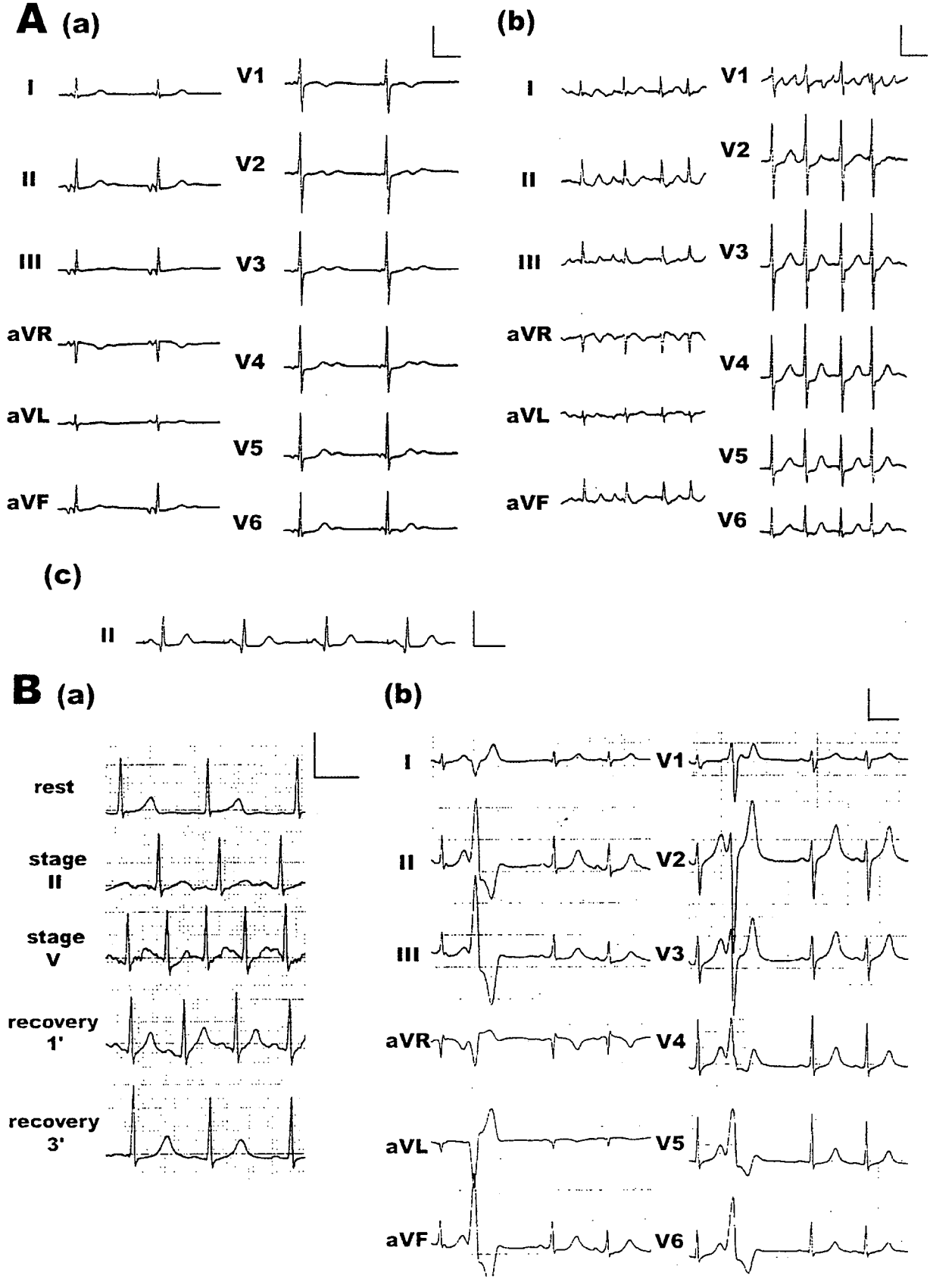

Figure 2 A: ECG of case 1: (a) 12-lead ECG at rest, (b) ECG showing AF, (c) lead II strip during atrial pacing at 60 bpm. B: ECGs in the case 2: (a) lead V5 strips in treadmill exercise test. With increasing exercise levels, the QT prolongation became more prominent. (b) Twelve-lead ECG at 3 minutes of recovery. Scale bars indicate 1 mV and 400 ms.

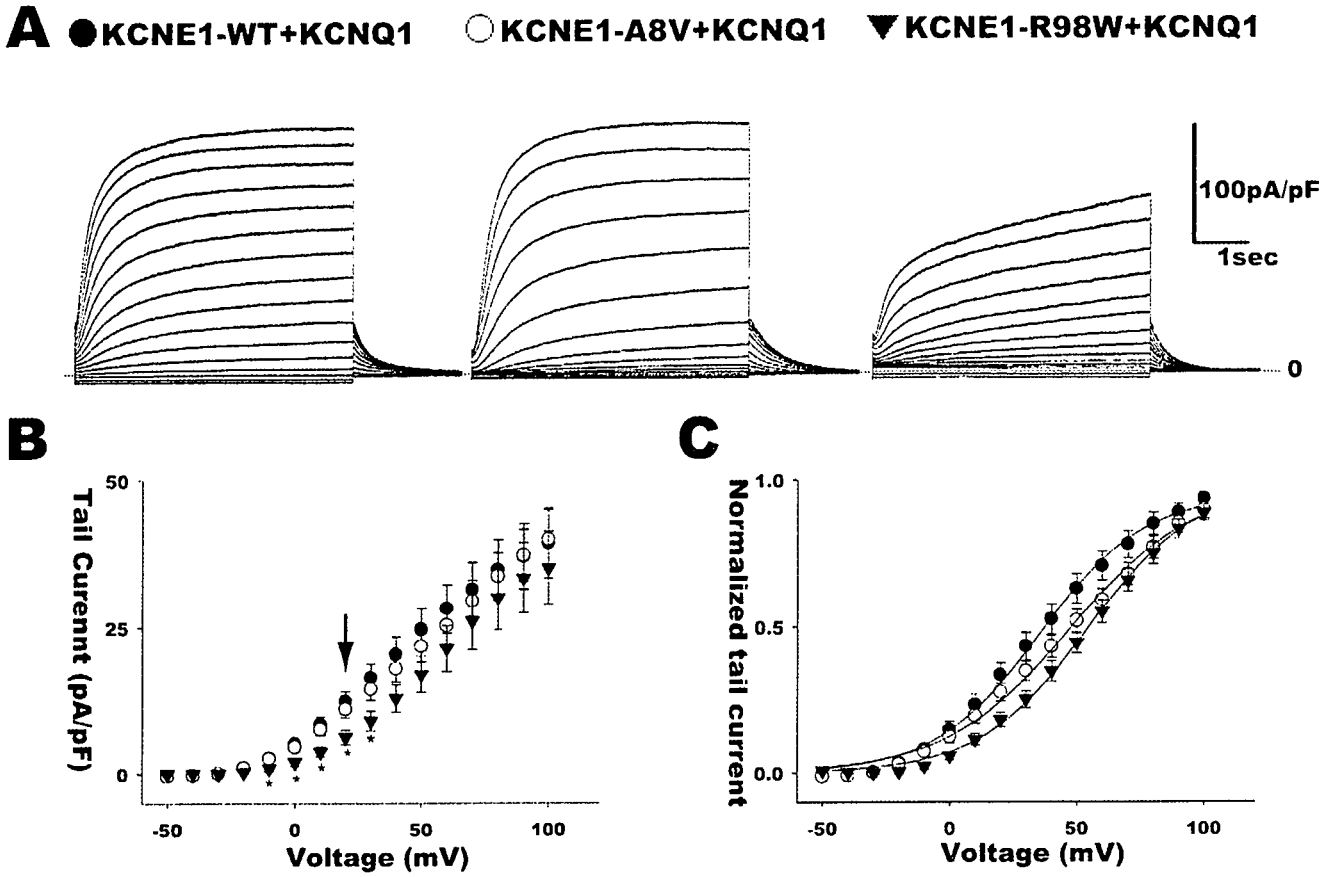

Figure 3 A: Current traces recorded from cells expressing *KCNE1*-WT, A8V or R98W with *KCNQ1*. Currents were elicited from a holding potential of −70 mV, by depolarizing pulses from −50 to +100 mV (with a10-mV step increment) and subsequent repolarization to −30 mV. **B:** Tail current voltage relations for *KCNE1*-WT/*KCNQ1* (*closed circles*, n = 16), A8V/*KCNQ1* (*open circles*, n = 17), and R98W/*KCNQ1* (*closed triangles*, n = 16). **P* <.05 versus WT and R98W. **C:** Normalized activation curves.

as a function of test potentials in Figure 4C, and each data set was fitted by equation 1. $V_{1/2}$ and k values were −19.5 ± 0.8 and 7.7 ± 0.4 mV for WT, −25.9 ± 0.8 and 7.9 ± 0.5 mV for A8V, and −19.8 ± 2.3 and 6.9 ± 0.4 mV for R98W, respectively. Therefore, A8V produced a negative shift of $V_{1/2}$ by 6 mV (P <.05 vs. WT). Time constants of deactivation were calculated by fitting to equation 3. τ_{fast} and τ_{slow} for tail currents at −60 mV after the +50 mV test pulse were 0.19 ± 0.04 and 1.16 ± 0.21 seconds for WT, 0.25 ± 0.03 and 1.61 ± 0.18 seconds for A8V, and 0.24 ± 0.02 and 1.58 ± 0.09 seconds for R98W, respectively. The values of these time constants did not differ significantly between cells expressing WT and mutant MinK.

Discussion

Clinical features of type 5 LQTS

In the present study, we identified two *KCNE1* mutations in two of 151 unrelated Japanese LQTS probands (1.3%). One of them, A8V, was novel and was identified in an elderly LQTS woman who had paroxysmal AF and sick sinus syndrome. Although her resting ECG displayed marked bradycardia and QT prolongation, her QT interval was normalized after atrial pacing therapy. Recently, *KCNE1* polymorphism (38G) has been shown to be associated with AF.[25] We also found the homozygous 38G allele in the patient, which may be related to her AF. Another mutation, R98W, was found in a young woman athlete who suffered from recurrent short-term syncope only during exercise. Although her ECG displayed only mild QTc prolongation (460 ms), subsequent exercise stress test revealed that her QTc lengthened markedly along with the heart rate increase. We therefore could not rule out the possibility that her symptoms were due to torsades de pointes. Although the R98W mutation has already been reported in an LQTS patient,[26] we could not compare the clinical features of the two cases because no clinical information is available from the previous study.[26]

We were unable to conduct extensive genetic assays for family members of these index patients, but based on their clinical data, both of our patients exhibited a mild LQTS. Biophysical assessment of the *KCNE1* mutants revealed that the newly identified A8V mutation affected significantly the magnitude of expressed *KCNH2* current, leading to a loss-of-function type modulation. Consistent with the functional measurements, our patient with heterozygous A8V mutations showed a definite bradycardia-dependent QT prolongation and sinus bradycardia. The I_{Kr} deactivation process has been implicated as an important part of the pacemaker

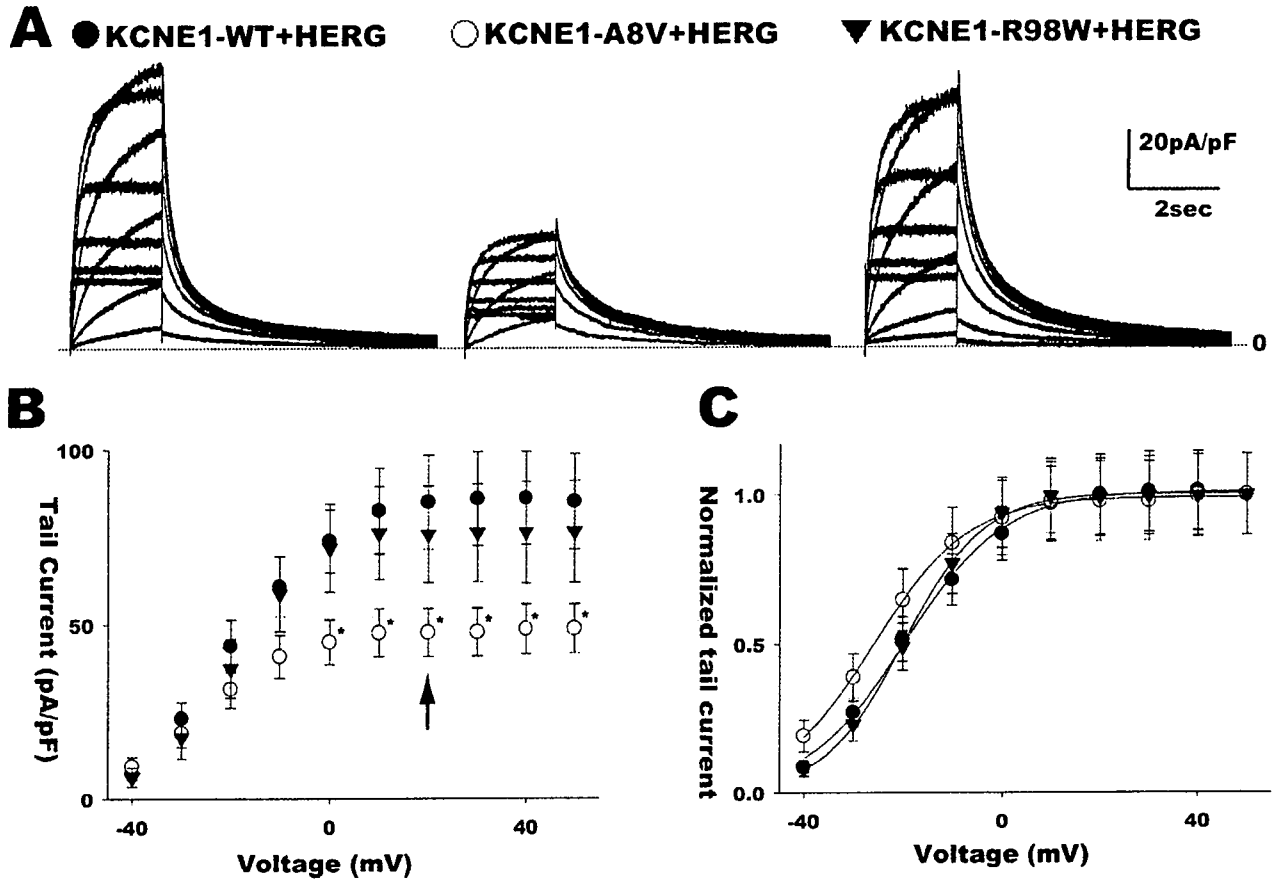

Figure 4 A: Current traces recorded from cells expressing *KCNE1*-WT, A8V, or R98W with *KCNH2*. They were elicited from a holding potential of −80 mV by application of depolarizing pulses from −40 to +50 mV (with a 10-mV step increment) and subsequent repolarization to −60 mV. **B:** Tail current voltage relations for *KCNE1*-WT/*KCNH2* (*closed circles*, n = 6), A8V/*KCNH2* (*open circles*, n = 9), and R98W/*KCNH2* (*closed triangles*, n = 8). $P < .05$ versus WT and A8V. **C:** Normalized activation curves.

mechanism,[27] and reduced I_{Kr} may lead to the sinus bradycardia. She had apparently no episodes of torsade de pointes, and her QT interval was normalized after pacing therapy. These features are indeed concordant with a type 2 rather than type 1 LQTS. In addition, our clinical observations suggest that *KCNE1* mutation may be associated with AF in this patient.

MinK encoded by *KCNE1* has been shown to form a stable complex with HERG protein in heterologous coexpression,[11] while MinK-antisense treatment has also been reported to affect I_{Kr} magnitude.[10] Considered together with our observations, this suggests that the A8V MinK mutation may cause a relatively mild LQTS phenotype as a consequence of an altered functional effect on the HERG channel protein. A previously reported *KCNE1* mutation (D76N) has been shown to influence the interaction of MinK with both the KCNQ1 and HERG proteins.[28] However, detailed information on the resulting phenotypes is not available, especially on the rate dependency of QT interval prolongation. To our knowledge, therefore, our A8V case is the first reported example of LQTS exhibiting the phenotype different from type 1 LQTS as a consequence of a *KCNE1* mutation.

Functional analyses of *KCNE1* mutations in N- and C-terminal regions

Until now, only 16 *KCNE1* mutations have been reported, and four of these were homozygous JLNS patients as listed in Table 1. Similar to our cases, Schulze-Bahr and colleagues[29] demonstrated that heterozygous *KCNE1* mutations displayed a relatively mild or even normal phenotype with very low penetrance. This may partially explain why *KCNE1* mutations are more frequently found among JLNS patients. It becomes clinically significant when *KCNE1* mutations produce a severe functional disturbance in a homozygous manner, thereby leading to the JLNS phenotype.

Among 16 *KCNE1* mutations, functional analyses are available on eight mutations (Table 1), four of which were located in the transmembrane segment and the rest in the C terminus. Tapper and George[30] reported that transmembrane and C terminal regions of *KCNE1* interact with the *KCNQ1* protein. Three *KCNE1* mutations in the N terminus have already been reported (T7I,[7] R32H,[26] and R36H[31]), but their functional outcome has not been examined. Alanine at codon 8 is next to threonine at 7[7] and caused a significant modulation on the MinK/HERG complex (Figure 4). Our data therefore raise the possibility that other

Table 1 Summary of all *KCNE1* mutations

Amino acid change	Protein domain	Phenotype	Reference
T7I	N terminal	JLNS*	7
A8V	N terminal	RWS	This study
R32H	N terminal	RWS	26
R36H	N terminal	RWS	31
V47H	Transmembrane	JLNS†	28
L51H	Transmembrane	JLNS†	28
G52R	Transmembrane	RWS	34
F53S	Transmembrane	RWS	31
T59P-L60P	Transmembrane	JLNS	35
K70N	Transmembrane	RWS	36
S74L	C terminal	RWS	8
D76N	C terminal	RWS/JLNS*	7
Y81C	C terminal	RWS	36
W87R	C terminal	RWS	28
R98W	C terminal	RWS	This study, 26
V109I	C terminal	RWS	29
P127T	C terminal	RWS	26

*T7I, D76N; compound heterozygous mutation.
†V47H, L51H; compound heterozygous mutation.

N-terminal mutations may also be of functional importance in the interaction with the HERG protein.

C-terminal *KCNE1* mutations caused various functional changes according to their location and the species of mutated amino acids: the D76N mutation displayed a dominant-negative effect, but S74L caused only current decrease.[8] In general, most C-terminal mutations produced a very mild functional change, and the dominant negative suppression was only seen in D76N. In our experiments, R98W caused a decrease in current density and a positive shift of the activation curve. Melman and colleagues[32] constructed chimeras of *KCNE1* and *KCNE3* and determined the region of *KCNE1* that is necessary and sufficient to modulate the *KCNQ1*. This appeared to be located in the transmembrane portion, which indicates that N- and C-terminal mutations caused no extreme change in I_{Ks} current. This may be one reason why most of the patients with LQT5 mutations in the C terminus showed the rather mild phenotype.

Study limitations

Considering the fact that we did not find any other discernible mutations in the known LQTS genes for the index patients, we employed DHPLC analysis to screen for genetic variants, which may not be 100% effective in the detection of mutations.[33] In DHPLC analysis, although the temperatures of the analysis are optimal, we may miss mutations in the very high or low melting domains. It also cannot be excluded that there might be mutations within regulatory regions or intronic sequences that are important for splicing or transcription.

Conclusion

We have identified two heterozygous mutations that manifested the mild phenotype of LQTS (1.3% incidences among LQTS probands). In the presence of additional risks such as hypokalemia and drugs associated with QT prolongation, however, the arrhythmia risk for these carriers could increase considerably. Therefore, the identification of *KCNE1* mutations with possible phenotypic effects in LQTS patients may be of significant value in providing information important for our understanding of LQT genotype-phenotype correlations. Moreover, in considering the basis for the functional consequences of such mutations, changes to HERG/I_{Kr} as well as KCNQ1/I_{Ks} need to be considered.

Acknowledgments

The authors are grateful to the Japanese LQT families for their willingness to participate in this study. We thank Dr. Andrew F. James, Bristol University, for reading the manuscript.

References

1. Moss AJ, Kass RS. Long QT syndrome: from channels to cardiac arrhythmias. J Clin Invest 2005;115:2018–2024.
2. Wang Q, Curran ME, Splawski I, Burn TC, Millholland JM, VanRaay TJ, Shen J, Timothy KW, Vincent GM, de Jager T, Schwartz PJ, Towbin JA, Moss AJ, Atkinson DL, Landes GM, Connors TD, Keating MT. Positional cloning of a novel potassium channel gene: KvLQT1 mutations cause cardiac arrhythmias. Nat Genet 1996;12:17–23.
3. Takumi T, Ohkubo H, Nakanishi S. Cloning of a membrane protein that induces a slow voltage-gated potassium current. Science 1988;242:1042–1045.
4. Murai T, Kakizuka A, Takumi T, Ohkubo H, Nakanishi S. Molecular cloning and sequence analysis of human genomic DNA encoding a novel membrane protein which exhibits a slowly activating potassium channel activity. Biochem Biophys Res Commun 1989;161:176–181.
5. Barhanin J, Lesage F, Guillemare E, Fink M, Lazdunski M, Romey G. K_vLQT1 and IsK (minK) proteins associate to form the I_{Ks} cardiac potassium current. Nature 1996;384:78–80.
6. Sanguinetti MC, Curran ME, Zou A, Shen J, Spector PS, Atkinson DL, Keating MT. Coassembly of KvLQT1 and minK (IsK) proteins to form cardiac I_{Ks} potassium channel. Nature 1996;384:80–3.
7. Schulze-Bahr E, Wang Q, Wedekind H, Haverkamp W, Chen Q, Sun Y, Rubie C, Hordt M, Towbin JA, Borggrefe M, Assmann G, Qu X, Somberg JC, Breithardt G, Oberti C, Funke H. *KCNE1* mutations cause Jervell and Lange-Nielsen syndrome. Nat Genet 1997;17:267–268.
8. Splawski I, Tristani-Firouzi M, Lehmann MH, Sanguinetti MC, Keating MT. Mutations in the hminK gene cause long QT syndrome and suppress I_{Ks} function. Nat Genet 1997;17:338–340.
9. Duggal P, Vesely MR, Wattanasirichaigoon D, Villafane J, Kaushik V, Beggs AH. Mutation of the gene for IsK associated with both Jervell and Lange-Nielsen and Romano-Ward forms of long-QT syndrome. Circulation 1998;97:142–146.
10. Yang T, Kupershmidt S, Roden DM. Anti-minK antisense decreases the amplitude of the rapidly activating cardiac delayed rectifier K^+ current. Circ Res 1995;77:1246–1253.
11. McDonald TV, Yu Z, Ming Z, Palma E, Meyers MB, Wang KW, Goldstein SA, Fishman GI. A minK-HERG complex regulates the cardiac potassium current I_{Kr}. Nature 1997;388:289–292.
12. Tamargo J, Caballero R, Gomez R, Valenzuela C, Delpon E. Pharmacology of cardiac potassium channels. Cardiovasc Res 2004;62:9–33.
13. Schwartz PJ, Moss AJ, Vincent GM, Crampton RS. Diagnostic criteria for the long QT syndrome. An update. Circulation 1993;88:782–784.
14. Splawski I, Shen J, Timothy KW, Vincent GM, Lehmann MH, Keating MT. Genomic structure of three long QT syndrome genes: *KVLQT1*, *HERG*, and *KCNE1*. Genomics 1998;51:86–97.
15. Neyroud N, Richard P, Vignier N, Donger C, Denjoy I, Demay L, Shkolnikova M, Pesce R, Chevalier P, Hainque B, Coumel P, Schwartz K, Guicheney P. Genomic organization of the KCNQ1 K^+ channel gene and identification of C-terminal mutations in the long-QT syndrome. Circ Res 1999;84:290–297.
16. Wang Q, Li Z, Shen J, Keating MT. Genomic organization of the human SCN5A gene encoding the cardiac sodium channel. Genomics 1996;34:9–16.

17. Abbott GW, Sesti F, Splawski I, Buck ME, Lehmann MH, Timothy KW, Keating MT, Goldstein SA. MiRP1 forms I_{Kr} potassium channels with HERG and is associated with cardiac arrhythmia. Cell 1999;97:175–187.
18. Mohler PJ, Schott JJ, Gramolini AO, Dilly KW, Guatimosim S, duBell WH, Song LS, Haurogne K, Kyndt F, Ali ME, Rogers TB, Lederer WJ, Escande D, Le Marec H, Bennett V. Ankyrin-B mutation causes type 4 long-QT cardiac arrhythmia and sudden cardiac death. Nature 2003;421:634–639.
19. Jongbloed R, Marcelis C, Velter C, Doevendans P, Geraedts J, Smeets H. DHPLC analysis of potassium ion channel genes in congenital long QT syndrome. Hum Mutat 2002;20:382–391.
20. Tesson F, Donger C, Denjoy I, Berthet M, Bennaceur M, Petit C, Coumel P, Schwarts K, Guicheney P. Exclusion of KCNE1 (IsK) as a candidate gene for Jervell and Lange-Nielsen syndrome. J Mol Cell Cardiol 1996;28:2051–2055.
21. Westenskow P, Splawski I, Timothy KW, Keating MT, Sanguinetti MC. Compound mutations: a common cause of severe long-QT syndrome. Circulation 2004;109:1834–1841.
22. Paulussen AD, Gilissen RA, Armstrong M, Doevendans PA, Verhasselt P, Smeets HJ, Schulze-Bahr E, Haverkamp W, Breithardt G, Cohen N, Aerssens J. Genetic variations of *KCNQ1*, *KCNH2*, *SCN5A*, *KCNE1*, and *KCNE2* in drug-induced long QT syndrome patients. J Mol Med 2004;82:182–188.
23. Denjoy I, Berthet M, Gouas L, Simon F, Lupoglazoff JM. A homozygous mutation in KCNE1 cause long-QT syndrome without deafness. Circulation 2004;110(Suppl 3):501.
24. Sanguinetti MC, Jiang C, Curran ME, Keating MT. A mechanistic link between an inherited and an acquired cardiac arrhythmia: *HERG* encodes the I_{Kr} potassium channel. Cell 1995;81:299–307.
25. Lai LP, Su MJ, Yeh HM, Lin JL, Chiang FT, Hwang JJ, Hsu KL, Tseng CD, Lien WP, Tseng YZ, Huang SK. Association of the human minK gene 38G allele with atrial fibrillation: evidence of possible genetic control on the pathogenesis of atrial fibrillation. Am Heart J 2002;144:485–490.
26. Splawski I, Shen J, Timothy KW, Lehmann MH, Priori S, Robinson JL, Moss AJ, Schwartz PJ, Towbin JA, Vincent GM, Keating MT. Spectrum of mutations in long-QT syndrome genes. *KVLQT1*, *HERG*, *SCN5A*, *KCNE1*, and *KCNE2*. Circulation 2000;102:1178–1185.
27. Ono K, Ito H. Role of rapidly activating delayed rectifier K+ current in sinoatrial node pacemaker activity. Am J Physiol 1995;269:H453–462.
28. Bianchi L, Shen Z, Dennis AT, Priori SG, Napolitano C, Ronchetti E, Bryskin R, Schwartz PJ, Brown AM. Cellular dysfunction of LQT5-minK mutants: abnormalities of I_{Ks}, I_{Kr} and trafficking in long QT syndrome. Hum Mol Genet 1999;8:1499–1507.
29. Schulze-Bahr E, Schwarz M, Hauenschild S, Wedekind H, Funke H, Haverkamp W, Breithardt G, Pongs O, Isbrandt D. A novel long-QT 5 gene mutation in the C-terminus (V109I) is associated with a mild phenotype. J Mol Med 2001;79:504–509.
30. Tapper AR, George AL Jr. MinK subdomains that mediate modulation of and association with KvLQT1. J Gen Physiol 2000;116:379–389.
31. Napolitano C, Priori SG, Schwartz PJ, Bloise R, Ronchetti E, Nastoli J, Bottelli G, Cerrone M, Leonardi S. Genetic testing in the long QT syndrome: development and validation of an efficient approach to genotyping in clinical practice. JAMA 2005;294:2975–2980.
32. Melman YF, Domenech A, de la Luna S, McDonald TV. Structural determinants of KvLQT1 control by the KCNE family of proteins. J Biol Chem 2001;276:6439–6444.
33. Xiao W, Oefner PJ. Denaturing high-performance liquid chromatography: a review. Hum Mutat 2001;17:439–474.
34. Ma L, Lin C, Teng S, Chai Y, Bahring R, Vardanyan V, Li L, Pongs O, Hui R. Characterization of a novel long QT syndrome mutation G52R-KCNE1 in a Chinese family. Cardiovasc Res 2003;59:612–619.
35. Tyson J, Tranebjaerg L, Bellman S, Wren C, Taylor JF, Bathen J, Aslaksen B, Sorland SJ, Lund O, Malcolm S, Pembrey M, Bhattacharya S, Bitner-Glindzicz M. IsK and KvLQT1: mutation in either of the two subunits of the slow component of the delayed rectifier potassium channel can cause Jervell and Lange-Nielsen syndrome. Hum Mol Genet 1997;6:2179–2185.
36. Lai LP, Su YN, Hsieh FJ, Chiang FT, Juang JM, Liu YB, Ho YL, Chen WJ, Yeh SJ, Wang CC, Ko YL, Wu TJ, Ueng KC, Lei MH, Tsao HM, Chen SA, Lin TK, Wu MH, Lo HM, Huang SK, Lin JL. Denaturing high-performance liquid chromatography screening of the long QT syndrome-related cardiac sodium and potassium channel genes and identification of novel mutations and single nucleotide polymorphisms. J Hum Genet 2005;50:490–496.

MUTATION IN BRIEF

Genotype-Phenotype Correlations of *KCNJ2* Mutations in Japanese Patients With Andersen-Tawil Syndrome

Yoshisumi Haruna[1†], Atsushi Kobori[1†], Takeru Makiyama[1], Hidetada Yoshida[1], Masaharu Akao[1], Takahiro Doi[1], Keiko Tsuji[2], Seiko Ono[1], Yukiko Nishio[1], Wataru Shimizu[3], Takehiko Inoue[4], Tomoaki Murakami[5], Naoya Tsuboi[6], Hideo Yamanouchi[7], Hiroya Ushinohama[8], Yoshihide Nakamura[9], Masao Yoshinaga[10], Hitoshi Horigome[11], Yoshifusa Aizawa[12], Toru Kita[1], and Minoru Horie[2*]

[1]Department of Cardiovascular Medicine, Kyoto University Graduate School of Medicine, Kyoto, Japan; [2]Department of Cardiovascular and Respiratory Medicine, Shiga University of Medical Science, Otsu, Japan; [3]Division of Cardiology, Department of Internal Medicine, National Cardiovascular Center, Suita, Japan; [4]Division of Child Neurology, Institute of Neurological Sciences, Faculty of Medicine, Tottori University, Yonago, Japan; [5]Department of Pediatrics, Hokkaido University Graduate School of Medicine, Sapporo, Japan; [6]Department of Cardiology, Nagoya Daini Red Cross Hospital, Nagoya, Japan; [7]Department of Pediatrics, Dokkyo University School of Medicine, Tochigi, Japan; [8]Pediatric Cardiology Division, Fukuoka Children's Hospital and Medical Center for Infectious Diseases, Fukuoka, Japan; [9]Department of Pediatric Cardiology, Japanese Red Cross Society Wakayama Medical Center, Wakayama, Japan; [10]National Hospital Organization Kyushu Cardiovascular Center, Kagoshima, Japan; [11]Department of Pediatrics, Institute of Clinical Medicine, University of Tsukuba, Tsukuba, Japan; [12]Department of Cardiology, Niigata University Graduate School of Medical and Dental Sciences, Niigata, Japan

[†]These authors equally contributed to this work.

*Correspondence to: Minoru Horie, MD, PhD, Department of Cardiovascular and Respiratory Medicine, Shiga University of Medical Science, Seta Tsukinowa-cho, Otsu, Shiga 520-2192, Japan; Tel.: +81-77-548-2213; Fax: +81-77-543-5839; E-mail: horie@belle.shiga-med.ac.jp

Grant sponsor: Dr Horie is supported in part by research grants from the Ministry of Education, Science, Sports and Culture of Japan (#16209025). Dr Aizawa and Dr Horie are supported by grants from Ministry of Health, Labor and Welfare for Clinical Research for Evidence Based Medicine. Dr W Shimizu is supported in part by Ministry of Education, Culture, Sports, Science and Technology Leading Project for Bio-simulation, and Health Sciences Research grants (H17 - Research on Human Genome, Tissue Engineering - 009) from the Ministry of Health, Labour and Welfare, Japan. Grant number: #16209025

Communicated by Johannes Zschocke

Andersen-Tawil syndrome (ATS) is a rare inherited disorder characterized by periodic paralysis, mild dysmorphic features, and QT or QU prolongation with ventricular arrhythmias in electrocardiograms (ECGs). Mutations of *KCNJ2*, encoding the human inward rectifying potassium channel Kir 2.1, have been identified in patients with ATS. We aimed to clarify the genotype-phenotype correlations in ATS patients. We screened 23

Received 30 January 2006; accepted revised manuscript 19 December 2006.

DOI: 10.1002/humu.9483

clinically diagnosed ATS patients from 13 unrelated Japanese families. Ten different forms of *KCNJ2* mutations were identified in the 23 ATS patients included in this study. Their ECGs showed normal QTc intervals and abnormal U waves with QUc prolongation and a variety of ventricular arrhythmias. Especially, bidirectional ventricular tachycardia (VT) was observed in 13 of 23 patients (57%). Periodic paralysis was seen in 13 of 23 carriers (57%), dysmorphic features in 17 (74%), and seizures during infancy in 4 (17%). Functional assays for the two novel *KCNJ2* mutations (c. 200G>A (p. R67Q) and c. 436G>A (p. G146S)) displayed no functional inward rectifying currents in a heterologous expression system and showed strong dominant negative effects when co-expressed with wild-type *KCNJ2* channels (91% and 84% reduction at –50 mV respectively compared to wild-type alone). Immunocytochemistry and confocal imaging revealed normal trafficking for mutant channels. In our study, all of the clinically diagnosed ATS patients had *KCNJ2* mutations and showed a high penetrance with regard to the typical cardiac phenotypes: predominant U wave and ventricular arrhythmias, typically bidirectional VT. © 2007 Wiley-Liss, Inc.

KEY WORDS: Andersen-Tawil syndrome; long QT syndrome; tachyarrhythmia; *KCNJ2*; ion channelopathy; potassium channels; bidirectional ventricular tachycardia; QU prolongation; periodic paralysis; dysmorphic features

INTRODUCTION

Andersen-Tawil syndrome (ATS, MIM# 170390) is a rare autosomal dominant disorder characterized by classical triad: (1) ventricular tachyarrythmias associated with QT prolongation in electrocardiograms (ECGs), (2) periodic paralysis, and (3) dysmorphic features (Andersen, et al., 1971; Canun, et al., 1999; Sansone, et al., 1997; Tawil, et al., 1994). Plaster et al. revealed that mutations in *KCNJ2* (MIM# 600681) caused the syndrome in the majority of clinically diagnosed ATS families (Plaster, et al., 2001). *KCNJ2* encodes a pore-forming subunit of inwardly rectifying potassium channels (Kir 2.1), a critical contributor for the I_{K1} current, which maintains normal resting membrane potentials and regulates the final phase of action potential repolarization in various types of cells (Kubo, et al., 1993; Raab-Graham, et al., 1994). To date, more than 30 *KCNJ2* mutations were identified and reported to be responsible for ATS (Ai, et al., 2002; Bendahhou, et al., 2005; Davies, et al., 2005; Donaldson, et al., 2003; Hosaka, et al., 2003; Plaster, et al., 2001; Tristani-Firouzi, et al., 2002; Zhang, et al., 2005). Most mutations in *KCNJ2* showed loss-of-function and dominant negative suppression effects (Tristani-Firouzi, et al., 2002), and a mutation, p.S136F, has been shown to suppress the native I_{K1} in neonatal rat cardiomyocytes (Lange, et al., 2003).

In contrast to the relatively homogenous change in functional outcome as a result of the mutations, ATS patients displayed a wide range of penetrance and severity of clinical phenotypes (Plaster, et al., 2001). This perplexity makes it difficult for physicians to properly diagnose the syndrome. Indeed, some cases have been diagnosed and treated as long QT syndrome (LQTS) and others as periodic paralysis. Tristani-Firouzi et al. performed extensive genetic and phenotypic analyses of ATS patients from 17 families and suggested that ATS might be classified as a new subtype of LQTS (referred to as *KCNJ2*-associated LQTS (LQT7)) (Tristani-Firouzi, et al., 2002). Recently, Zhang et al. reviewed the ECGs of 96 ATS patients with *KCNJ2* mutations and revealed the median QTc interval in ATS patients to be within the normal range (Zhang, et al., 2005). They concluded that *KCNJ2*-associated ATS is not a subtype of LQTS and recommended to have them annotated as ATS1. In a study on guinea pig hearts transfected with a dominant negative *KCNJ2* mutant, Miake et al. demonstrated that suppression of I_{K1} decelerated the action potential repolarization, prolonged the action potential duration, and depolarized the resting membrane potential. They also observed that the suppression of I_{K1} caused QTc prolongation on surface ECGs.

In order to clarify the genotype-phenotype correlations in Japanese ATS patients, we carried out a complete screening of *KCNJ2* in 23 ATS patients and investigated their clinical manifestations.

METHODS

Study Subjects

Twenty-three clinically diagnosed Japanese ATS patients (from 13 unrelated families) were enrolled in this study from 12 institutes in Japan. Individuals were diagnosed as being affected with ATS if 2 or 3 of the following criteria were present: (1) episodes of muscle weakness, (2) cardiac involvement, and/or (3) dysmorphology as previously described (Donaldson, et al., 2003; Tristani-Firouzi, et al., 2002). The presence of periodic paralysis was based on standard criteria (McManis, et al., 1986). Cardiac involvement was determined by the presence of ventricular arrhythmias (frequent premature ventricular contractions (PVCs), bigeminy, ventricular tachycardia (VT)), prolongation of the corrected QT interval (QTc) and/or a prominent U wave. Subjects were classified as having QT prolongation if the QTc exceeded 440 milliseconds (ms) for males and 460 ms for females, in accordance with standard criteria (Keating, et al., 1991). The QT interval was defined from the onset of QRS to the end of the T wave. The U wave was defined as an early diastolic deflection after the end of the T wave. The QU interval was defined from the onset of QRS to the end of the U wave. QT and QU intervals were corrected according to Bazzett's formula (Bazzett, 1920; Zhang, et al., 2005). The end of the T or U wave was the point at which a tangent drawn to the steepest portion of the terminal part of the T or U wave crossed the isoelectric line (Yan and Antzelevitch, 1998). Because a prominent U wave is fused to the next PQ segment in some cases, we defined the isoelectric line as a segment connecting two points preceding consecutive QRS complexes. Abnormal U waves were judged by the following criteria: (a) wave amplitude $\geq$ 0.2 mV (Lepeschkin, 1972) or (b) amplitude larger than preceding T wave (Lepeschkin, 1969).

Dysmorphology was defined by the presence of 2 or more of the following: (a) low-set ears, (b) hypertelorism (wide-set eyes), (c) small mandible, (d) clinodactyly (permanent lateral or medial curve of a finger or toe), and (e) syndactyly (persistent webbing between fingers or toes) (Tristani-Firouzi, et al., 2002).

In order to elucidate the genetic differences between ATS and LQTS, we also screened *KCNJ2* mutations in 74 LQTS probands from 74 unrelated families. They displayed no clinical signs compatible with ATS except for cardiac manifestations.

DNA Isolation and Mutation Analysis

The protocol for genetic analysis was approved by the Institutional Ethics Committee and was performed under its guidelines. All patients provided an informed consent before the genetic analysis was carried out. Genomic DNA was isolated from leukocyte nuclei using a DNA extraction kit, QIAamp DNA Blood midi kit, (QIAGEN GmbH, Hilden, Germany). Genetic screening for *KCNJ2* was performed by polymerase chain reaction/single-strand conformation polymorphism (PCR-SSCP) analysis (Yoshida, et al., 1999) or denaturing high-performance liquid chromatography (DHPLC) using WAVE System Model 3500 (Transgenomic, Omaha, NE, USA) (Ning, et al., 2003). Abnormal conformers were amplified via PCR, and sequencing was performed on an ABI PRISM3100 DNA sequencer (Applied Biosystems, Wellesley, MA, USA). The cDNA sequence numbering was based upon GenBank reference sequence NM_000891.2 for *KCNJ2* and NM_000218.2 for *KCNQ1* (the first adenosine in the initiator ATG was designed as +1).

In Vitro Mutagenesis

With regard to the novel *KCNJ2* mutations, site-directed mutagenesis was employed to construct mutants as described previously (Hosaka, et al., 2003). Briefly, human *KCNJ2* cDNA was subcloned into the pCMS-EGFP plasmid (Clontech, Palo Alto, CA, USA). We engineered *KCNJ2* mutants using a site-directed mutagenesis kit, QuickChange II XL (Stratagene, La Jolla, CA, USA). The presence of mutations was confirmed by sequencing.

Electrophysiological Experiments and Data Analysis

To assess the functional modulation of *KCNJ2* channels, we employed a heterologous expression system with COS7 cells (Kubota, et al., 2000). Briefly, the cells were transiently transfected by the LipofectAMINE method as directed in the manufacture's instructions (Invitrogen, Carlsbad, CA, USA), using a 1.0 μg/35 mm dish of pCMS-EGFP/*KCNJ2* (wild type (WT) and/or mutant). For electrophysiological experiments, GFP-positive cells were selected 24 to 72 hours after transfection. Current measurement was conducted by the conventional whole-cell configuration of patch-clamp techniques at 37°C, using an Axopatch 200A patch clamp amplifier and a Digidata 1322A digitizer (Axon Instruments, Foster City, CA, USA). pClamp software (version 9.0, Axon Instruments)

was used to generate voltage pulse protocols and for data acquisition. Currents were evoked by 150 ms square pulses applied in 10 mV increments to potentials ranging from –140 mV to +30 mV from a holding potential of –80 mV. Pipettes were filled with a solution containing (in mM): K-aspartate 60, KCl 65, KH_2PO_4 1, $MgCl_2$ 2, EDTA 3, K_2ATP 3 and HEPES 5 adjusted to pH 7.4 using KOH, and had a resistance of 3.0 to 5.0 MΩ. The bath solution contained (in mM): NaCl 140, KCl 5.4, $MgCl_2$ 0.5, $CaCl_2$ 1.8, NaH_2PO_4 0.33, glucose 5.5, and HEPES 5 (pH 7.4 with NaOH) (Yoshida, et al., 1999). All the data are shown as mean ± SEM. Where appropriate, Student's unpaired *t*-test was used; a value of $P < 0.05$ was considered statistically significant.

Immunocytochemistry

The hemaggulutinin (HA) epitope (YPYDVPDVA) was introduced into the pCMS-EGFP/*KCNJ2* (WT and mutants) between Ala-115 and Ser-116 (extracellular lesion between TM1 and TM2) as previously described (Ballester, et al., 2006). COS7 cells were transfected with 1.0 μg of plasmid DNA in 35 mm glass-bottom dishes. Forty-eight hours later, the cells were washed twice with phosphate buffered saline (PBS), followed by incubation with a mouse anti-HA primary antibody (1:500) (Covance Research Products, Inc., Berkeley, CA, USA) for 30 minutes at 37°C. The cells were then washed twice with PBS and incubated with an anti-mouse antibody conjugated to the Alexa 594 fluorophor (1:500) (Molecular Probes, Eugene, OR, USA) as a secondary antibody for 30 minutes at 37°C. Finally, cells were washed with and immersed in PBS, and confocal imagings were obtained with a Zeiss LSM 510 (Carl Zeiss GmbH, Jena, Germany).

RESULTS

***KCNJ2* Mutation Analysis**

Figure 1 and Table 1 show the mutations and clinical findings of 23 ATS patients (9 males/14 females; mean 23.0 ± 3.1 years old). There were 13 probands from 13 unrelated families. We found 10 different heterozygous *KCNJ2* mutations (two were novel) in the 23 ATS patients examined in this study: c.199C>T (p.R67W) (Andelfinger, et al., 2002); c.200G>A (p.R67Q); c.430G>A (p.G144S) (Kobori, et al., 2004); c.436G>A (p.G146S); c.574A>G (p.T192A) (Ai, et al., 2002); c.644G>A (p.G215D) (Hosaka, et al., 2003); c.652C>T (p.R218W) (Plaster, et al., 2001); c.653G>A (p.R218Q) (Tristani-Firouzi, et al., 2002); c.899G>T (p.G300V) (Tristani-Firouzi, et al., 2002); and c.926C>T (p.T309I) (Bendahhou, et al., 2005). R67Q and G146S were novel mutations. Arginine at codon 67 is implicated in binding membrane-associated phoshatidylinositol 4,5-bisphosphate (PIP_2), and has been reported to be a hot spot for ATS mutations (Donaldson, et al., 2003; Zhang, et al., 2005), but the substitution of arginine with glutamine (R67Q) is a novel mutation. G146S is also a novel mutation located at an essential region known as the K^+ channel signature sequence that serves as a principal ion selective filter (Doyle, et al., 1998). Therefore, both R67Q and G146S are supposed to cause substantial effects to *KCNJ2* channels.

In 8 kindred (K-024, K-037, K-178, K-180, K240, K-323, KJ-01, and KJ-02, Table 1) the mutations were inherited from parents. In contrast, they were *de novo* in 3 probands of 3 kindred (K-179, K-201, and K-324) and were undetermined in 2 kindred (N-01 and KJ-03) because detailed family information was not available. These *KCNJ2* variants were not present in 100 normal controls (200 alleles). Analysis for other known LQTS-responsible genes (*KCNQ1*, *KCNH2*, *SCN5A*, *KCNE1*, and *KCNE2*) revealed that K-024 proband and her son were also heterozygous for a *KCNQ1* mutation (c.1022C>T (p.A341V))(Kobori, et al., 2004).

In 74 LQTS patients, we found one novel *KCNJ2* variant (c.1051C>T (p.P351S)) in a 74-year-old female who had suffered from syncope and received a pacemaker implantation. In addition, genetic analysis had revealed that she was a carrier of c.1927G>A (p.G643S) (*KCNQ1*). This variant (P351S-*KCNJ2*) could not be identified in 100 healthy controls.

The cDNA sequence numbering was based upon GenBank reference sequence NM_000891.2 for *KCNJ2* and NM_000218.2 for *KCNQ1* (the first adenosine in the initiator ATG was designed as +1).

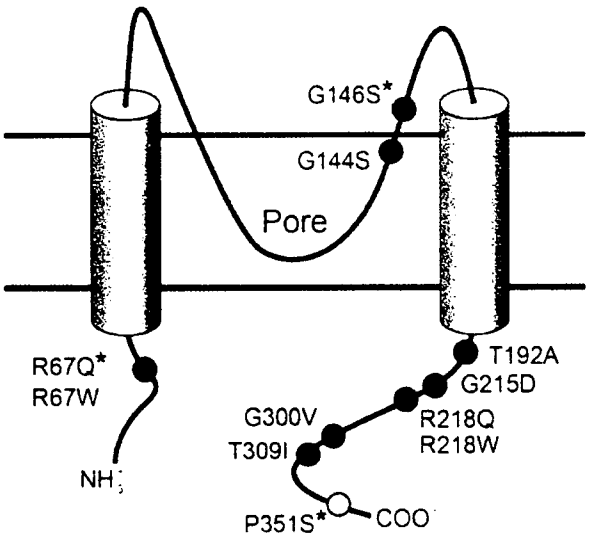

Figure 1. Topology of the Kir 2.1 channel. Scheme showing the topology of the Kir 2.1 channel and the location of 10 *KCNJ2* mutations (filled circles) found in 23 ATS and 1 (open circle) in a LQTS patient. Asterisks indicate novel mutations.

General Clinical Findings

Table 1 summarizes ECG findings and two other major phenotypes in 23 ATS patients. Seven of the 23 mutation carriers (30 %) showed the full clinical triad, and 16 (70 %) had two of the three phenotypes.

Cardiac Manifestations (Table 1 and Fig. 2)

In 2 cases (G146S: a proband, and T309I: a proband), it was difficult to measure the RR interval and recognize the U wave because of very frequent premature contractions and sustained ventricular bigeminy. Two G144S patients had A341V-*KCNQ1* mutation. We therefore excluded these 4 cases from ECG parameter analyses. In the remaining 19 cases, the mean QTc interval was 406 ± 10 ms, and only 3 (16%) had a QTc ≥ 460 ms. Based on the criteria described in Methods, 16 patients (84%) showed abnormal U waves (Fig. 2A-C and Table 1). Their serum K^+ concentrations were within normal range. There were no other factors influencing the U wave formation such as bradycardia or drugs.

Ventricular tachyarrhythmias were observed in 15 patients (65%; 12 of 13 probands and 3 of 10 family members): monomorphic VT in 2 (9%), polymorphic VT in 4 (17%), bidirectional VT in 13 (57%) (Fig. 2D), and ventricular fibrillation (VF) in one (4%).

β blockers (propranolol, atenolol, metoprolol, or carvedilol) were prescribed for 7 individuals, calcium channel blocker (verapamil) for 5 and sodium channel blockers (one is flecainide, the others are mexiletine) for 3. These drugs appeared to prevent cardiac events effectively in each case.

Periodic Paralysis

Periodic paralysis was observed in 13 patients (57%). In some of them, muscle weakness was triggered by elevated fever, exercise, and menstruation. Biopsy of skeletal muscle demonstrated tubular aggregates in 2 probands (Ai, et al., 2002; Hosaka, et al., 2003). Carbonic anhydrase inhibitors prevented or reduced the attack in 4, however, they were not effective in 2 cases.

Table 1 **Characteristics of *KCNJ2* Mutation Carriers**

No. of kindred	Mutation in *KCNJ2*		Age	Sex	Cardiac Manifestations							Paralysis	Dysmorphology	Symptom	Seizure	Therapy
	cDNA	Protein			HR (bpm)	QTc (ms)	QUc (ms)	T amplitude (mV)	U amplitude (mV)	Tp-Up (ms)	U/T[††]	Ventricular Arrhythmia					
KJ-01	199C>T	R67W*	30	F	68	383	766	0.60	0.15	240	0.25	a, b, d	+	+	-	-	-
	199C>T	R67W	55	F	71	479	761	0.30	0.15	200	0.50	-	-	+	-	-	-
	199C>T	R67W	20	F	93	430	647	0.15	0.30	200	2.00	b, c	-	+	-	-	-
K-323	200G>A	R67Q*	13	F	54	360	626	1.10	0.30	232	0.27	a, c, d	-	+	Syncope	-	Carvedilol, Mexiletine
K-024	430G>A	G144S[†]*	36	F	67	480	803	0.40	0.30	280	0.75	a, d, f	+	+	Syncope	-	Propranorol, Verapamil, K
	430G>A	G144S[†]	11	M	70	460	756	NA	NA	250	NA	b, d	-	+	Aborted SD	+	Propranorol, Verapamil
K-179	436G>A	G146S*	28	F	126[†††]	N	NA	NA	NA	NA	NA	a, b, d, f	+	+	-	-	Atenolol
K-037	574A>G	T192A*	13	M	89	487	731	0.30	0.32	208	1.07	a, b	+	-	-	+	Acetazolamide
	574A>G	T192A	11	F	86	431	790	0.66	0.22	280	0.33	a, f	+	-	-	-	Acetazolamide
N-01	644G>A	G215D*	34	F	73	408	794	0.78	0.33	280	0.42	a, b, f, g	+	+	Aborted SD	-	ICD
K-180	652C>T	R218W*	6	F	80	483	716	0.05	0.15	200	3.00	a, b, c, d, e	+		Syncope	+	Flecainide
	652C>T	R218W	38	M	54	384	693	0.80	0.20	250	0.25	a	+	-	-	+	-
	652C>T	R218W	73	M	52	410	670	0.50	0.25	220	0.50	-	+	-	-	-	-
K-240	652C>T	R218W*	11	F	78	365	758	0.30	0.35	240	1.17	b, c, d, e	-	+	-	-	Mexiletine
	652C>T	R218W	47	M	91	394	640	0.45	0.20	240	0.44	-	-	+	-	-	-
	652C>T	R218W	5	M	78	342	684	0.30	0.15	220	0.50	b, c	-	+	Myalgia	-	-
K-324	652C>T	R218W*	6	M	82	339	701	0.14	0.20	255	1.43	a, c, d	+	+	-	-	Verapamil
K-178	653G>A	R218Q*	13	F	60	420	700	0.40	0.20	220	0.50	b, c, d	+	+	-	-	-
	653G>A	R218Q	42	M	55	402	651	0.80	0.28	230	0.35	b	+	-	-	-	-
K-201	653G>A	R218Q*	12	F	105	423	741	0.65	0.40	200	0.62	b, c, d	+	+	Palpitation	-	-
KJ-02	899G>T	G300V*	16	M	103	393	786	0.90	0.30	240	0.33	b, d	-	+	Syncope	-	Propranorol, Verapamil
	899G>T	G300V	36	F	67	444	740	0.45	0.30	240	0.67	a, b, c, d	-	+	Syncope	-	Propranorol, K
KJ-03	926C>T	T309I*	17	F	NA	NA	NA	NA	NA	NA	NA	a, b, c, d	-	+	Malaise	-	Metoprolol, Verapamil
			23 ± 3.1		77 ± 4.1	406 ± 10	715 ± 12	0.51 ± 0.07	0.25 ± 0.02	231 ± 5.6	0.76 ± 0.16						

Table 1. Characteristics of *KCNJ2* mutation carriers. *: proband. †: compound heterozygous *KCNQ1*(c.1022C>T (p.A341V)) mutation carrier. ††: U/T means the ratio of U amplitude compared to T amplitude. †††: Because this patient had frequent extra ventricular systoles, heart rate was recorded as 126 bpm. NA: nonavailable information. As for ventricular arrhythmias, a: PVC, b: bigeminy, c: couplet, d: bidirectional VT, e: monomorphic VT, f: polymorphic VT, g: VF. SD: sudden cardiac death. As for treatments, K indicates potassium supplement, and ICD: implantable cardioverter defibrillator. The cDNA sequence numbering was based upon GenBank reference sequence NM_000891.2 for *KCNJ2*, NM_000218.2 for *KCNQ1* (the first adenosine in the initiator ATG was designed as +1).

Dysmorphology

Dysmorphology was observed in 17 patients (74%). Mandibular micrognathia (small mandible) was most frequently observed (11; 48%). Short stature was found in 8 (35%); clinodactyly in 6 (26%); hypertelorism in 6 (26%); low-set ears in 5 (22%); broad forehead in 4 (17%); and scoliosis in 1 (4%).

Other Manifestations in ATS Patients

Interestingly, 4 patients (17%) had episodes of afebrile seizures during infancy. Because Kir 2.1 channels are known to be distributed in various types of cells—including major parts of the brain (Raab-Graham, et al., 1994)—seizures as an episodic electrical phenotype of the central nervous system could be a clinical sign of ATS. Mild thyroid dysfunction was observed in one case.

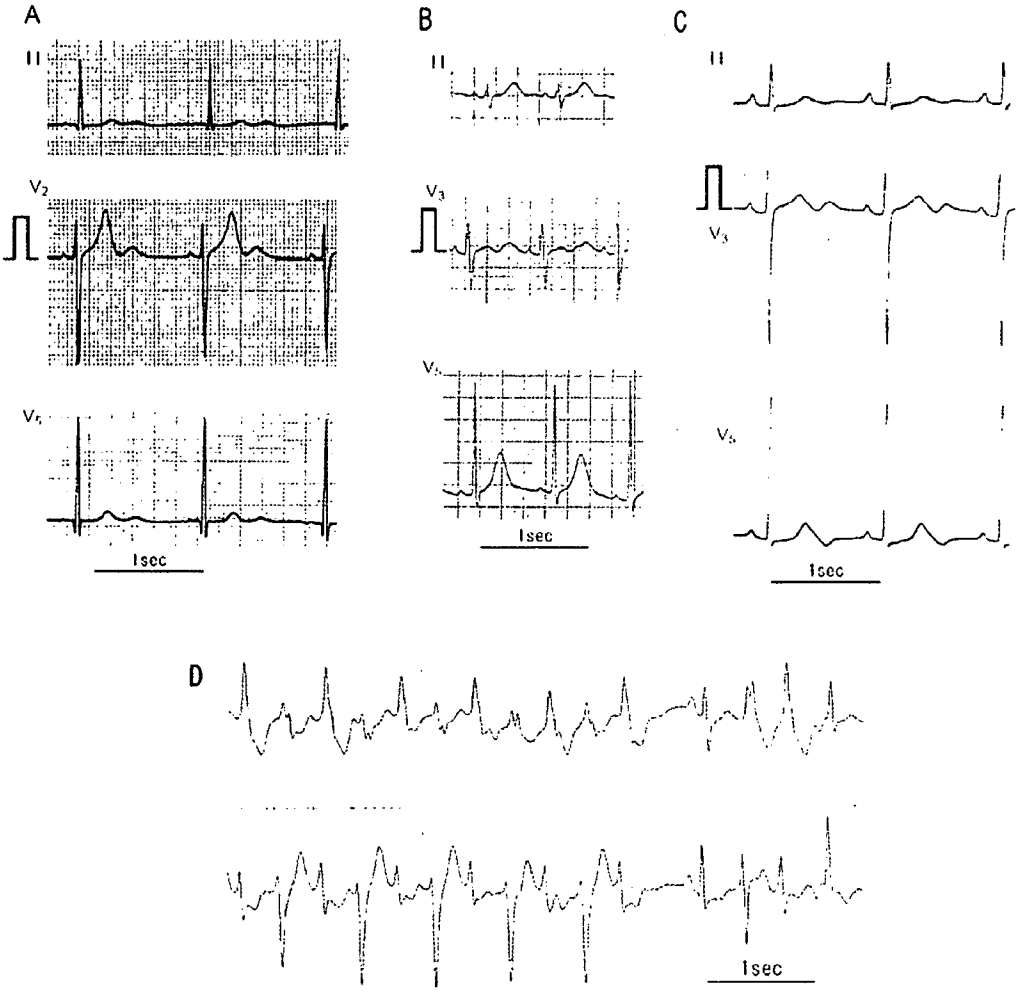

Figure 2. Representative ECG traces of *KCNJ2* mutation carriers. **A:** Normal QTc (360 ms) and abnormal U wave (U amplitude 0.30 mV) (K-323, R67Q). **B:** Normal QTc (373 ms) and abnormal U wave (U amplitude 0.30 mV and U amplitude > T amplitude) (KJ-01, R67W). **C:** QTc prolongation (460 ms) and abnormal U wave (U amplitude 0.30 mV) (K-024, Carrier of compound mutation A341V-*KCNQ1* and G144S-*KCNJ2*). **D:** bidirectional ventricular tachycardia in a Holter recording (K-179, G146S).

Electrophysiological Functional Assays

R67Q and G146S-*KCNJ2* Channels

We performed biophysical assays for the two novel *KCNJ2* mutations using the whole-cell patch clamp method in COS7 cells.

COS7 cells transfected with WT-*KCNJ2* cDNA (1 μg/dish: Fig. 3A-a) displayed K^+ currents with a strong inward rectification, which are typical of I_{K1} as previously described (Kubo, et al., 1993; Raab-Graham, et al., 1994). However, neither of the mutants—R67Q nor G146S—displayed measurable currents when transfected alone (Fig. 3A-b,c).

To simulate the allelic heterozygosity, WT and each mutant-*KCNJ2* were co-transfected at an equimolar ratio (0.5 μg/dish, respectively, Fig. 3A-d,e). Panel B of Figure 3 shows current-voltage relations. The currents co-expressed of WT with either mutant-*KCNJ2* showed the inward rectification. As summarized in bar graphs of Figure 3C, current densities for co-expression of WT-*KCNJ2* with R67Q (white bar) or G146S (gray bar) were –123 ± 32 pA/pF and –157 ± 23 pA/pF at –140 mV, and –9 ± 6 pA/pF and –15 ± 5 pA/pF at –50 mV, respectively. They were significantly smaller than those displayed by WT (–362 ± 48 pA/pF at –140 mV and 94 ± 16 pA/pF at –50 mV, indicated by closed bars). Both mutants showed a larger suppression at –50 mV, which is more physiological membrane potential.

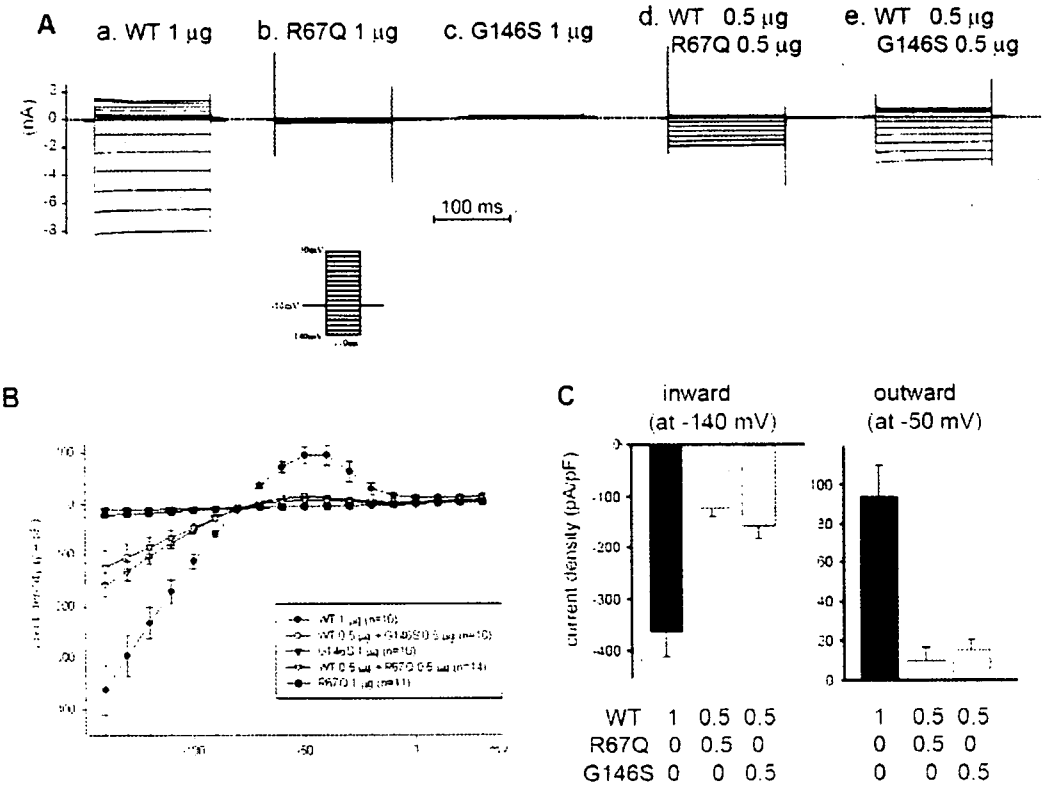

Figure 3. Both R67Q-*KCNJ2* and G146S-*KCNJ2* exert dominant negative effects on wild type function. **A:** Representative Kir 2.1 currents expressed in COS7 cells: (a) wild type (WT) cDNA 1 μg, (b) R67Q 1 μg, (c) G146S 1 μg, (d) co-transfection with WT 0.5 μg and R67Q 0.5 μg and (e) co-transfection with WT 0.5 μg and G146S 0.5 μg. Holding potential was set at –80 mV. Square pulses of 150 ms duration were applied to the potentials between –140 mV and +30 mV with a 10 mV increment. Time scale is given in the middle of graph. **B:** Plots for current-voltage relationships obtained by multiple experiments of the same protocol as shown in A. Current densities were calculated by dividing with cell capacitance. **C:** Bar graphs showing mean current densities in WT (black bars), co-transfection with WT and R67Q

(white bars) and co-transfection with WT and G146S (gray bars): left panel: those at –140 mV and right panel: those at –50 mV. Vertical bars indicate SEM.

P351S-*KCNJ2* Channel

We found one novel *KCNJ2*-variant (P351S) among 74 LQTS probands (1.4%). Functional assays revealed that the mutant channel displayed inwardly rectifying currents of similar size (Fig. 4A). In a heterozygous condition (Fig. 4B), the current densities of WT and WT/P351S were –362 ± 48 pA/pF and –350 ± 38 pA/pF at –140 mV, and 90 ± 15 pA/pF and 94 ± 20 pA/pF at –50 mV, respectively. Student *t*-tests revealed these changes in current were not significant. These findings suggested that the P351S-*KCNJ2* was a non-pathological variant associated with the LQT1 patient who lacked extra-cardiac signs of ATS.

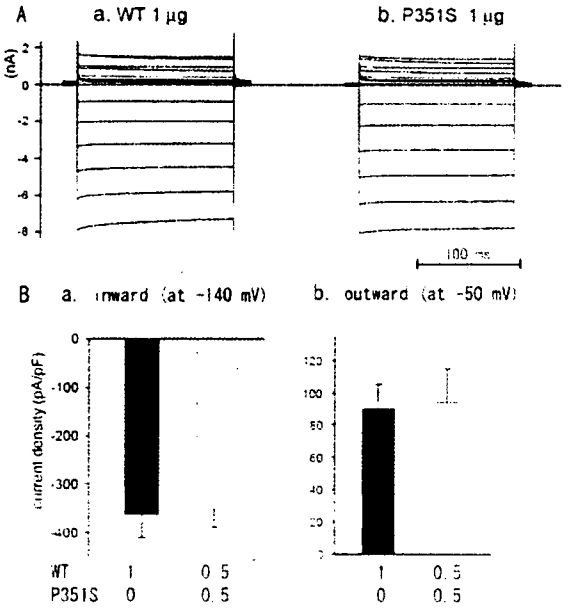

Figure 4. The Kir 2.1 variant in LQTS displays inwardly rectifying currents, which are indistinguishable from that of the WT. **A:** Representative Kir 2.1 currents expressed in COS7 cells: (a) WT cDNA 1 μg, (b) P351S 1 μg. Pulse protocols were the same in Fig. 3. **B:** Bar graphs showing averaged current densities induced by WT (black) and co-transfection of WT/P 351S (white) at test of (a) –140 mV and (b) –50 mV (n=8 respectively).

Immunocytochemistry of Mutant Channels (R67Q and G146S)

In order to investigate whether the R67Q and G146S mutations affect *KCNJ2* trafficking, immunocytochemistry and confocal imaging of mutant channels was performed. An HA tag was introduced into an extracellular loop lesion of *KCNJ2* in the pCMS-EGFP vector which carried GFP as a reporter gene. The HA-tagging procedure itself did not affect the functional expression of inwardly rectifying I_{K1} currents (data not shown).

Figure 5 illustrates typical results of confocal imaging. COS7 cells were transfected with HA-*KCNJ2*, HA-R67Q, HA-G146S and *KCNJ2* (without HA tag)(Fig 5, upper panel). All of HA-tagged *KCNJ2* (HA-*KCNJ2*, HA-R67Q and HA-G146S) exhibited red fluorescence at the plasma membrane (Fig 5, middle panel), indicating that both R67Q and G146S were trafficking-competent mutants.

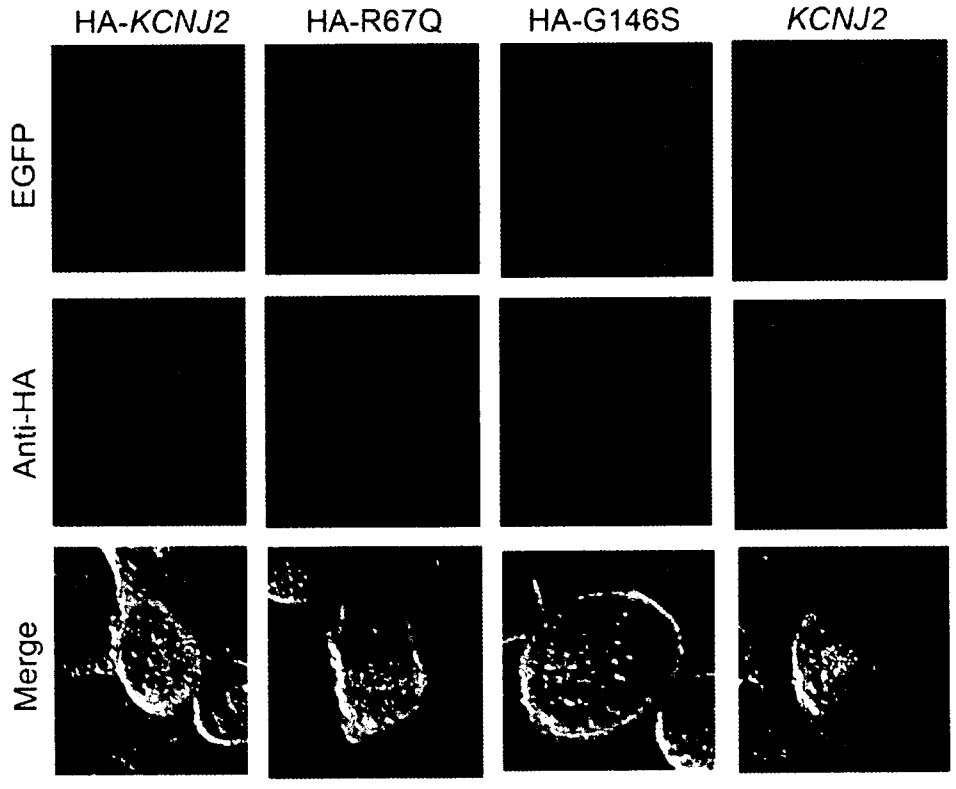

Figure 5. Cellular localization of WT and mutant Kir 2.1 channels. In figure, HA-*KCNJ2* indicates HA-tagged WT-*KCNJ2* (positive control), *KCNJ2*; WT-*KCNJ2* without HA tagging (negative control), and HA-R67Q and HA-G146S; HA-tagged mutant *KCNJ2*. Upper panel shows green fluorescence of GFP, middle panel; red fluorescence of secondary anti-HA antibody, bottom panel; merge of green fluorescence, red fluorescence, and transmission.

DISCUSSION

ATS is a rare inherited disorder characterized by periodic paralysis, mild dysmorphic features, and QT or QU prolongation with ventricular arrhythmias in ECGs. Mutations of *KCNJ2* have been identified in patients with ATS (ATS1). However, about 20-30% of clinically diagnosed ATS patients do not have the *KCNJ2* mutation (Plaster, et al., 2001; Tristani-Firouzi, et al., 2002; Zhang, et al., 2005), suggesting genetic heterogeneity. In the present study, we screened 23 clinically diagnosed ATS patients and identified 10 variations of *KCNJ2* mutations (including 2 novels, R67Q and G146S). Every genotyped patient had one of these 10 mutations. Therefore, all were ATS1 patients. As in our study, a recent genetic survey conducted in the UK (Davies, et al., 2005) demonstrated that all 11 probands from 11 unrelated ATS families were *KCNJ2*-positive (100% ATS1). Our findings, along with that of the UK, seem to contradict the prevalence rate mentioned above, however, ATS is a rare disorder and we should await future studies.

With regard to the cardiac manifestation of ATS, the mean QTc interval was within normal range (406 ± 10 ms), and only 3 of 19 cases (16%) showed prolonged QT intervals. In contrast, abnormal U waves were present in the majority (80%), thereby causing a markedly prolonged QUc interval (715 ± 12 ms). Although ATS had been suggested as a subtype of LQTS (LQT7), Zhang et al. showed the median QTc interval was within the normal range in 96 *KCNJ2*-positive ATS patients and suggested that the QTc prolongation reported in earlier studies was

due to the inclusion of U waves in the QT measurement. Our study supported their conclusion, and *KCNJ2*-positive ATS should be classified as ATS1 but not LQT7. In most patients, QTc intervals were within normal range, and the QTc prolongation was observed in only 3 pure ATS patients and 2 ATS patients with compound *KCNQ1* mutation (K-024) (Data of these two compound mutation patients were not included in the analysis of ECG parameters as described above). In our study, if cardiac manifestations were defined as abnormal U waves and/or ventricular arrhythmias, the penetration of cardiac manifestations was up to 96% (22 of 23).

The clinical severity of ventricular arrhythmias was reported to be milder in ATS than other subtypes of LQTS (Plaster, et al., 2001); however, 2 unrelated patients in our cohort experienced aborted sudden death (Hosaka, et al., 2003; Kobori, et al., 2004). Aborted sudden deaths have also been reported in the past (Junker, et al., 2002). It is much too early to conclude that arrhythmias in ATS are, for the most part, benign. Further studies are required to determine long-term prognosis, risk stratification for life threatening cardiac phenotypes, and for effective treatment.

Afebrile seizures were noted during infancy in 4 of 23 ATS patients (17%). This episodic electrical disorder related to the central nervous system was previously reported in one ATS patient having tonic clonic seizures associated with vomiting (Canun, et al., 1999). In our patients with a history of seizures, there were no identified fundamental conditions, including elevated fever, electrolyte abnormality, and/or organic central nervous system disorders. As for a possible mechanism underlying the seizures, Neusch and coworkers (Neusch, et al., 2003) demonstrated that reduced K^+ conductance induced by Kir mutants would disturb the clearance of external K^+ by glial cells during neuronal activities. Therefore, the impaired spatial K^+ buffering induced stronger and prolonged depolarization of glial cells and neurons in response to activity-dependent K^+ release, which may generate the seizures. Furthermore, the Kir current density has been noted to be reduced in temporal lobe epilepsy (Bordey and Sontheimer, 1998; Schroder, et al., 2000). It remains, however, unknown why these patients experienced the seizures only during infancy.

Subsequent functional assays for novel *KCNJ2* mutations (R67Q and G146S) revealed that they were non-functional and trafficking-competent mutations. In a heterozygous condition, they both caused strong dominant negative suppression effects (91% and 84% reduction at −50 mV respectively) (Fig. 3). These biophysical properties may be compatible with pathological roles in expression of ATS phenotypes as well as other mutations previously reported (Lange, et al., 2003).

In conclusion, Japanese ATS patients were exclusively associated with *KCNJ2* mutations (100% ATS1) and presented a high penetrance of cardiac manifestations (96%). ATS1 is a disorder distinct from LQTS. The disease entity is more characterized by a normal QTc interval, abnormal U waves and ventricular arrhythmias, typically bidirectional VT.

REFERENCES

Ai T, Fujiwara Y, Tsuji K, Otani H, Nakano S, Kubo Y, Horie M. 2002. Novel KCNJ2 mutation in familial periodic paralysis with ventricular dysrhythmia. Circulation 105(22):2592-4.

Andelfinger G, Tapper AR, Welch RC, Vanoye CG, George AL, Jr., Benson DW. 2002. KCNJ2 mutation results in Andersen syndrome with sex-specific cardiac and skeletal muscle phenotypes. Am J Hum Genet 71(3):663-8.

Andersen ED, Krasilnikoff PA, Overvad H. 1971. Intermittent muscular weakness, extrasystoles, and multiple developmental anomalies. A new syndrome? Acta Paediatr Scand 60(5):559-64.

Ballester LY, Benson DW, Wong B, Law IH, Mathews KD, Vanoye CG, George AL, Jr. 2006. Trafficking-competent and trafficking-defective KCNJ2 mutations in Andersen syndrome. Hum Mutat 27(4):388.

Bazzett HC. 1920. An analysis of the time relationships or time-relations of electrocardiograms. Heart 7:353-380.

Bendahhou S, Fournier E, Sternberg D, Bassez G, Furby A, Sereni C, Donaldson MR, Larroque MM, Fontaine B, Barhanin J. 2005. In vivo and in vitro functional characterization of Andersen's syndrome mutations. J Physiol 565(Pt 3):731-41.

Bordey A, Sontheimer H. 1998. Properties of human glial cells associated with epileptic seizure foci. Epilepsy Res 32(1-2):286-303.